The Southern Oscillation and Indonesian Sea Surface Temperature

N. NICHOLLS

Australian Numerical Meteorology Research Centre, Melbourne, Australia

(Manuscript received 5 July 1983, in final form 12 December 1983)

ABSTRACT

The relationship of the Southern Oscillation and El Niño phenomena to sea surface temperature anomalies in the Indonesian region is investigated. The three are closely related and the relationship has a strong annual cycle. The Indonesian sea surface temperature anomalies show strong persistence approximately from January through October with a tendency to dissipate or change sign around November. Changes of Indonesian sea surface temperature anomalies lead by about a season changes in the Southern Oscillation and east Pacific sea surface temperature.

It is demonstrated that a simple *ad hoc* model representing a stochastically-forced, seasonally-varying interaction between the atmosphere and the ocean in the Indonesian region can produce simulated anomalies of Darwin pressure and Indonesian sea surface temperature that reproduce the observed statistical behavior of these anomalies without the inclusion of the effects of oceanic and atmospheric events external to the Indonesian region. It suggested that the El Niño–Southern Oscillation might be the dynamic response of the Pacific Ocean and overlying atmosphere to anomalies produced by such an interaction in the Indonesian region. A speculation is raised involving the possible physical basis for such an interaction.

1. Introduction

The Southern Oscillation (SO) is a large-scale pattern of climate fluctuations, centered on the Pacific, but related to climatic events over much of the globe (Philander, 1983). The occasional warmings of the east equatorial Pacific Ocean, known as El Niño, are also associated with the SO (Rasmusson and Carpenter, 1982). The entire phenomenon is sometimes labeled the El Niño–Southern Oscillation, or ENSO. Over the past decade, some progress has been made toward understanding the causes of some features of ENSO. In particular, it has become clear that the El Niño sea surface temperature (SST) warmings in the east equatorial Pacific can be explained largely as the result of rapid horizontal redistributions of heat in the upper ocean in response to anomalous weakening of the trade winds over the west equatorial Pacific (Wyrtki, 1975, 1979; Barnett, 1983; McCreary, 1976; Hurlburt *et al.*, 1976; Busalacchi and O'Brien, 1981).

The cause of the anomalous weakening of the west equatorial Pacific easterlies is, however, not known. Other aspects of the ENSO are also poorly understood. Two features of considerable interest are the typical time scale of the anomalies (about a year) and their relationship to the annual cycle. Onset, intensification and collapse of anomalies in meteorological and oceanic variables associated with the SO are phase-locked to the annual cycle (Philander, 1983; Barnett, 1983).

A number of models of the ENSO phenomenon, with a variety of rather simple models of air–sea interaction, have been developed in an attempt to reproduce the observed time scales of the ENSO anomalies (e.g., McWilliams and Gent, 1978; Wright, 1979; McCreary, 1983). These models have demonstrated that some form of air–sea interaction can produce anomalies with time scales of several years. They have not, however, explained why the ENSO anomalies are so closely tied to the annual cycle, although Wright (1979) did observe that a seasonally varying feedback between the atmosphere and ocean could result in such a relationship.

These modeling efforts have concentrated on reproducing El Niño-like anomalies in the east equatorial Pacific, where the SST anomalies are most spectacular. Most recent empirical studies of the ENSO have also concentrated on the Pacific basin. Less work has been done to model or even examine the relationship of SST anomalies in the Indonesian region with ENSO. This is not surprising because these anomalies are much smaller than the anomalies in the east Pacific. Nevertheless, Indonesian SST's are strongly related to ENSO, in a complex, seasonally varying fashion (Berlage, 1957; Newell *et al.*, 1982). This relationship between SST anomalies in the east Pacific and Indonesian regions is illustrated in Fig. 1 which shows three-month running means of composite SST anomalies in the two regions for four El Niño events—1965, 1969, 1972 and 1976. The Indonesian SST's are the average for the area 5–15°S, 120–160°E while the east Pacific SST's come from La Punta/Callao (12°04'S,77°10'W).

The composites in Fig. 1 show that large anomalies of Indonesian SST accompany and precede the oc-

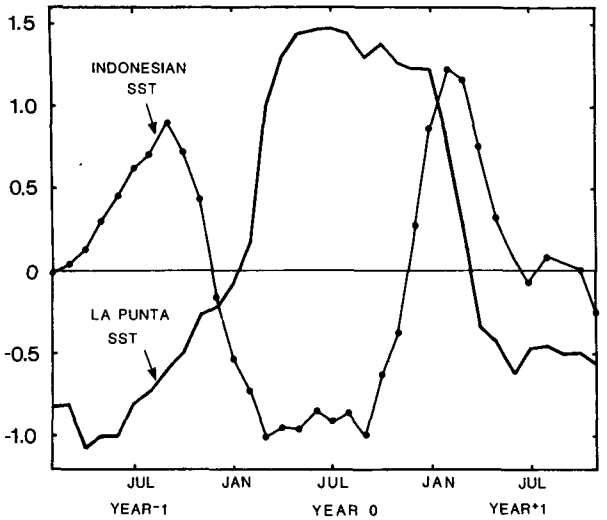

FIG. 1. Three-month running mean composites of Indonesian and La Punta/Callao SST anomalies in El Niño years (1965, 1969, 1972, 1976). Anomalies standardized by dividing by the standard deviation. Standardized anomalies greater in magnitude than 0.98 are significant at the 5% level.

currence of east Pacific SST anomalies associated with El Niño. The anomalies in Fig. 1 have been standardized by dividing by the standard deviation. El Niño tends to be preceded by warm SST anomalies in the Indonesian region which decrease rapidly and change sign around November, some months before the appearance of warm SST anomalies on the South American coast. The Indonesian SST's drop to a minimum by March and then show a strong warming trend from October onward. This rapid warming is followed several months later by a strong weakening of the El Niño SST anomalies. Thus, the changes in the sign of the Indonesian SST anomalies precede by several months the changes in sign of the east Pacific El Niño anomalies.

This study further examines the nature of this relationship between Indonesian SST and ENSO and speculates upon its possible cause.

2. Indonesian SST and the Southern Oscillation

In this section, the relationship of Indonesian SST to the SO is described. Darwin pressure is used as an index of the SO. Two SST datasets are used. The first is the 25-year (1913–37) set of monthly SST anomalies on the route from Bima (8°S, 119°E) to Makassar (5°S, 119°E) listed by Schregardus (1938). The second SST dataset, provided by P. B. Wright, is the SST anomaly averaged over the area 5–15°S, 120–160°E, from 1964 to 1982. Prior to 1964, these data were poor with many months of no observations.

It is also demonstrated here that a very simple *ad hoc* model of a stochastically-forced, seasonally-varying feedback between the atmosphere and ocean in the Indonesian region can simulate the observed statistical behavior of both Indonesian SST and Darwin pressure. The model is *ad hoc* to the extent that it has been developed specifically to reproduce this behavior.

The model can be represented by the following pair of coupled difference equations:

$$P(t+1) = \alpha P(t) - \beta T(t) + R, \quad (1)$$

$$T(t+1) = \alpha T(t) + \beta \cos(2\pi t/360) P(t) + R, \quad (2)$$

where $\alpha = 0.99$ and $\beta = 0.0125$.

In these equations, t represents time (days), where for simplicity the "year" consists of 12 months each of 30 days. Here, P and T represent standardized, unitless anomalies of pressure and SST in the Indonesian–north Australian region. The time step is one day and R represents a random number drawn from a uniform distribution between −0.1 and 0.1. A separate random number is drawn for each of the two above equations at each time step. The magnitudes of P and T produced by these equations are arbitrary.

The constants in the model (α and β) were selected so that the simulated anomalies reproduced observed atmospheric and oceanic behavior. The aspects, described below, of the behavior of the time series reproduced by the model, however, are rather robust with regard to changes in the constants.

The model is similar to one suggested by Nicholls (1979) as representing a form of air–sea interaction in the Indonesian–north Australian region capable of reproducing the observed behavior of atmospheric and oceanic anomalies in this area. The only difference of consequence is the use of a cosine function, rather than a step function, to represent the seasonally-varying effect of P on T [Eqs. (1) and (2)].

Initial values of zero were used for P and T at $t = 0$ and the equations solved for time steps of one day for a number of years. The first 20 years of simulated data produced by the model were used in the following analysis. Use of later periods of simulated data produces similar results. Monthly averages of P calculated in this way are plotted in Fig. 2a, and can be compared with a 20-year series of monthly mean anomalies of observed Darwin pressure (Fig. 2b). It should be noted here that Fig. 2a is *not* intended to reproduce Fig. 2b. Rather, the statistical behavior of P in Fig. 2a is intended to simulate that of Darwin pressure. For instance, Fig. 2a shows considerable periods, of the order of a year, for which the simulated pressure anomalies remain either positive or negative (e.g., years 7 and 8). Similar behavior is observed in the time series of Darwin pressure (e.g., 1972 and 1973). Also notable in Fig. 2 is the tendency for the anomalies, simulated and observed, to reach maximum amplitude toward the end of the calendar year and to rapidly change sign early in the year.

In the following subsections, serial and cross cor-

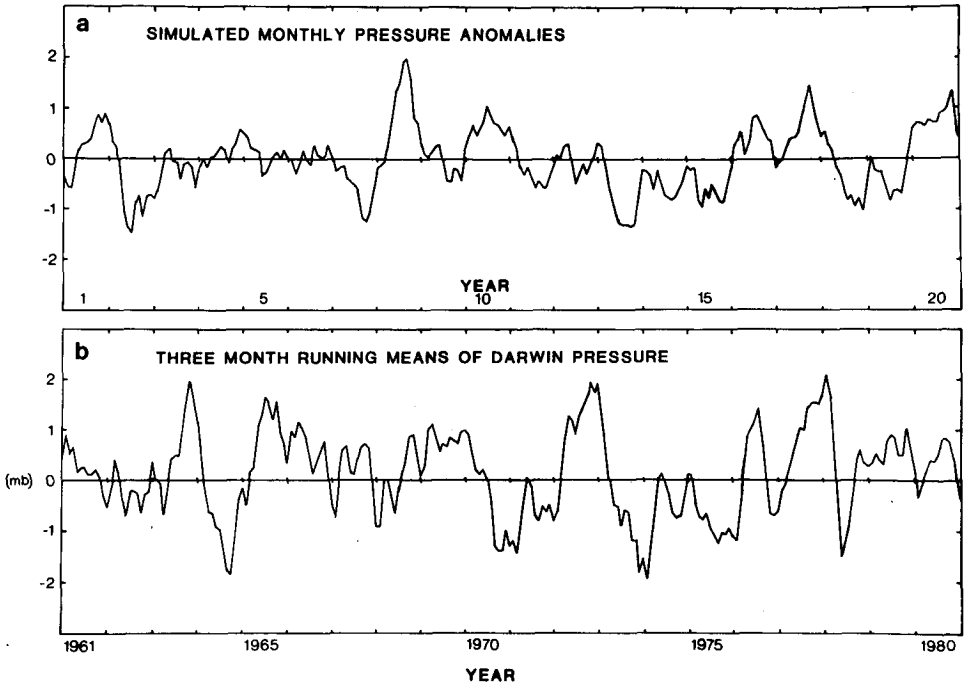

FIG. 2. (a) Monthly means of simulated pressures. (b) Three-month running means of anomalies of Darwin pressure. Data from 1960–80. January of each year is marked on axis.

relations and standard deviations of seasonal mean anomalies of observed and simulated SST and pressure anomalies are compared. All the correlations have been calculated with between 17 and 24 years of data, and serial correlations at a year lag were generally small, indicating reasonable independence from one year to the next. Thus, correlation coefficients greater in magnitude than 0.48 are assumed to be significant at the 5% level. Spectra of monthly mean anomalies are also presented.

a. Serial correlations of SST and pressure

The serial correlations of seasonal anomalies of Indonesian SST are shown in Fig. 3. Here, and in Figs. 5 and 6, the correlations calculated from observed data are shown as solid lines (1913–37 data) or as crosses (1964–82 data). The dashed lines in Figs. 3–8 represent correlations, standard deviations or spectra calculated from simulated anomalies produced by the model.

In Fig. 3, and also in Figs. 4–6, correlations at lags from −4 seasons to +4 seasons have been shown. The correlations have been calculated using each of the four seasons as the base season. Thus, Fig. 3 shows correlations of SST in the season indicated in the top left-hand corner of each of the four portions of the diagram, with the SST in seasons up to four seasons earlier or later.

The correlations demonstrate the existence of generally strong persistence from season to season. The

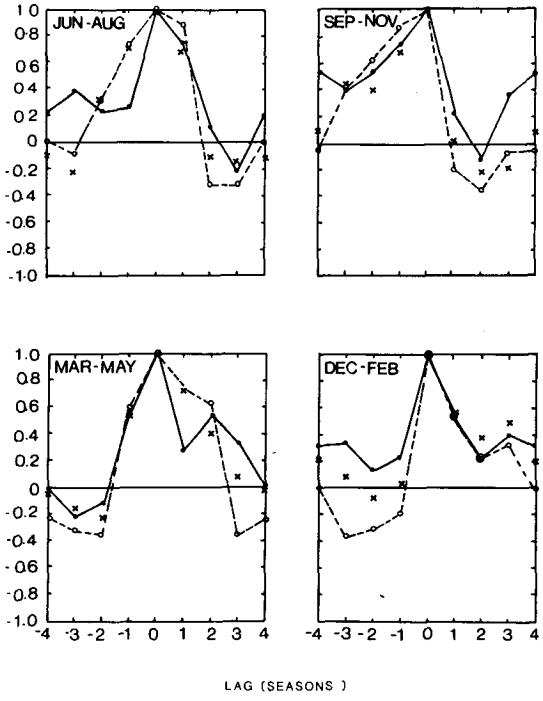

FIG. 3. Serial correlations of seasonal mean anomalies of Indonesian SST and of simulated SST. The base season is indicated in top left-hand corner of each section of the diagram. Lag, in season, is indicated. Correlations have been calculated from 1913–37 data (solid lines) and from 1964–80 data (crosses). The dashed lines indicate correlations calculated from the simulated values of SST.

correlation between SST anomalies in June–August and those in September–November (i.e., a lag of +1 season) is 0.75 in 1913–37 and 0.70 in 1964–82. There is also a clear variation in the pattern of the serial correlations through the year. SST anomalies tend to persist from December–February through to September–November, with less persistence from September–November to December–February, i.e., a greater tendency for changes in the anomaly to occur around November or December rather than at other times of the year.

The similarity of the lag correlations in Fig. 3 from two independent periods provides evidence of the stability and reality of the correlations.

The serial correlations of the simulated anomalies (dashed lines) reproduce the observed behavior, including the seasonal variations, quite well.

The seasonal serial correlations for Darwin pressure, calculated from 1961–80 data, are shown in Fig. 4. Again, generally strong persistence of the anomalies is apparent and a seasonal variation in the pattern of serial correlations of the seasonal pressure anomalies is also evident. The seasonal variation, however, is different from that in the SST correlations. The picture that emerges from the serial correlations of pressure is one of persistence of anomalies from March–May onward, with little persistence between December–February and March–May, i.e., a stronger tendency for anomalies to reverse or dissipate around February or March than at other times of the year.

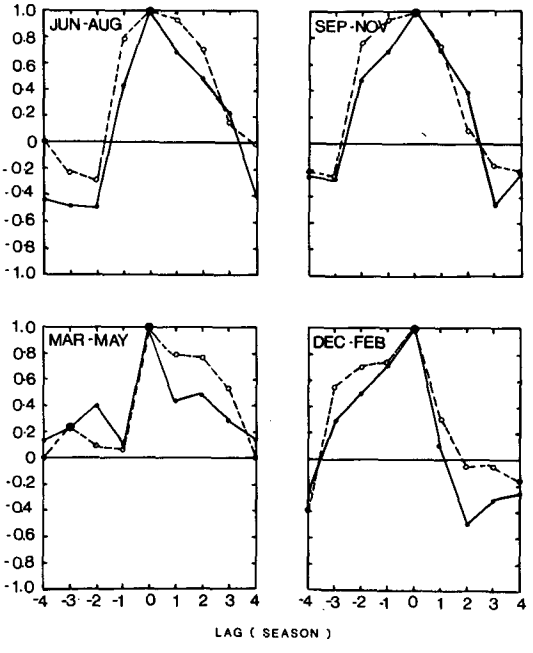

FIG. 4. As in Fig. 3 except for Darwin pressure and simulated pressures. The base season and lag are indicated. Correlations have been calculated from 1960–80 observed data (solid lines). Dashed line shows correlations calculated from simulated values of pressure.

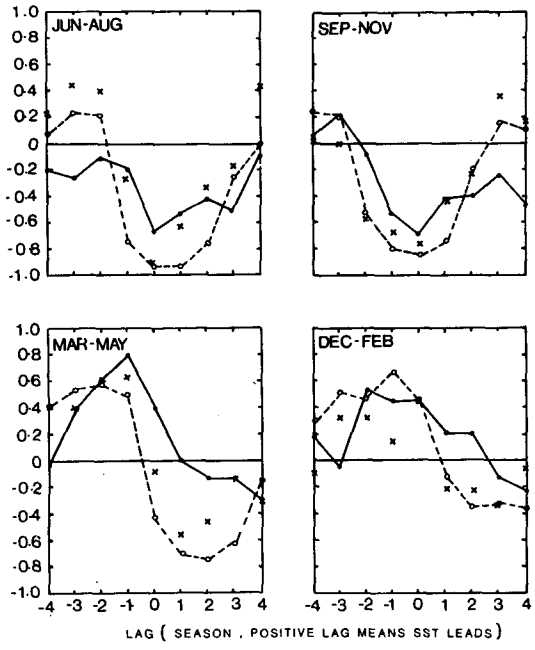

FIG. 5. Cross correlations between Indonesian SST in season indicated and Darwin pressure in earlier and later seasons. Positive lag means SST leads. Correlations have been calculated from 1913–37 data (solid lines) and from 1964–82 data (crosses). Also shown are the analagous cross correlations between simulated pressures and SSTs.

The information in Fig. 4 confirms earlier results, on earlier data, of Priestley (1962) and Troup (1965) who noted that February and March were the seasons when the persistence of Darwin pressure anomalies broke down.

Again, there is general correspondence between the serial correlations of the simulated pressure (dashed lines) and those of observed Darwin pressure. Overall, the simulated series adequately reproduce the observed serial correlations of both pressure and SST anomalies in the Indonesian–north Australian region.

b. Cross correlations of SST and pressure

The lag cross correlations of Indonesian SST and Darwin pressure have been calculated on data from 1913–37 and 1964–82. The results are shown in Fig. 5 for each season. The base month for the calculations is indicated for each section of Fig. 5 and the correlations of SST in that season with Darwin pressure up to four seasons earlier (negative lags) and up to four seasons later (positive lags) are plotted. As before, the correlations calculated from the model-simulated anomalies are shown as dashed lines.

Consider first the observed zero lag, i.e., simultaneous, correlations between SST and Darwin pressure. These correlations are substantial in each season and reach large magnitude (~0.7) during June–August and September–November. In March–May and Decem-

ber–February, the magnitudes are smaller. The correlations are negative in June–August and September–November and positive in December–February and March–May. Berlage (1957), using the 1913–37 dataset, has already noted this seasonal variation in correlation. Newell *et al.* (1982) also noted a seasonal variation in the sign of the correlation between an index of the SO and Indonesian SST, using data from 1861–1960 (their Fig. 3).

The observed lag cross correlations in Fig. 5 also vary with season. March–May SST is positively correlated with Darwin pressure in the previous three seasons. The magnitude of the correlation reaches a maximum with pressure in the previous December–February (lag = −1). The correlations at positive lags (i.e., with pressure in seasons after March–May) are zero or negative. This behavior should be contrasted with the pattern of correlations for the other seasons in Fig. 5.

The correlations shown in Fig. 5 are shown again in Fig. 6, but this time the diagrams are drawn to show correlations of Darwin pressure in the indicated season with SST up to four seasons earlier (negative lags) or later (positive lag). This rearrangement more clearly illustrates some of the seasonal variations in the cross correlations.

The cross correlations for the simulated data generally reproduce the observed correlations (Figs. 5 and 6). At zero lag, the cross correlations in June–August and September–November are negative, while in December–February they are positive, for both simulated and observed series. In March–May, however, the simulated series produce a negative cross-correlation whereas a positive or weak negative correlation is observed.

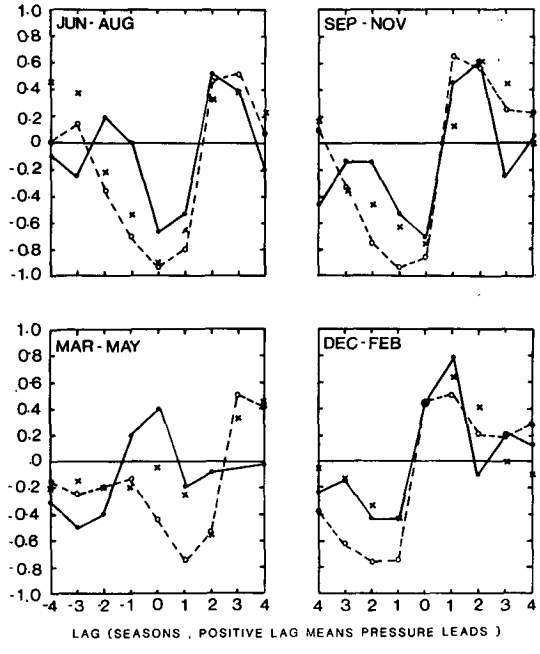

FIG. 6. As in Fig. 5 but with correlations rearranged so that indicated season is the base season for pressure. The correlations plotted are pressure in the indicated season with SST in earlier or later seasons. Positive lag means pressure leads.

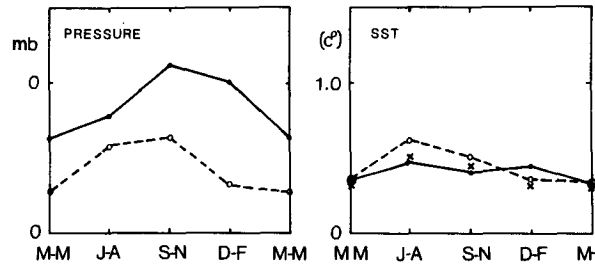

FIG. 7. Standard deviations of seasonal means of Darwin pressure in 1960–80 and Indonesian SST in 1913–37 (solid lines), Indonesian SST in 1964–82 (crosses), and simulated values of pressure and SST (dashed lines).

The cross correlations at nonzero lags are also similar in pattern and magnitude in the observed and simulated series.

c. Standard deviations of SST and Darwin pressure

Standard deviations of seasonal average anomalies of SST and Darwin pressure have been calculated, using the data involved in preparing Figs. 3 and 4 (Fig. 7). Considerable variation over the year of the variability of seasonal anomalies is evident. Thus, the greatest interannual variability of pressure is in September–November, with the lowest variability in March–May. Trenberth (1984) has calculated the standard deviations of Darwin pressures using a longer series of data (1941–80) and found the greatest variability in December–February rather than September–November. He also found the lowest variability in March–May. The strongest interannual variability of SST occurs in June–August (Fig. 7).

The patterns of the annual cycle in standard deviations of the simulated data are quite similar to those of Darwin pressure and Indonesian SST. Thus, the maximum variability of simulated pressure is found in September–November, with a minimum in March–May. On the other hand, the maximum variability in simulated SST occurs in June–August, as observed.

d. Spectra

Spectra of monthly anomalies of Darwin pressure and of simulated pressure anomalies from 1961 to 1982 are shown in Fig. 8. Each spectrum was calculated from 256 months of data. Both spectra show the concentration of power between 18 months and 10 years characteristic of the SO (Troup, 1965; Trenberth, 1976; Chen, 1982). The observed spectrum exhibits more power at high frequencies (not shown in Fig. 8) than does the simulated series and therefore contains more

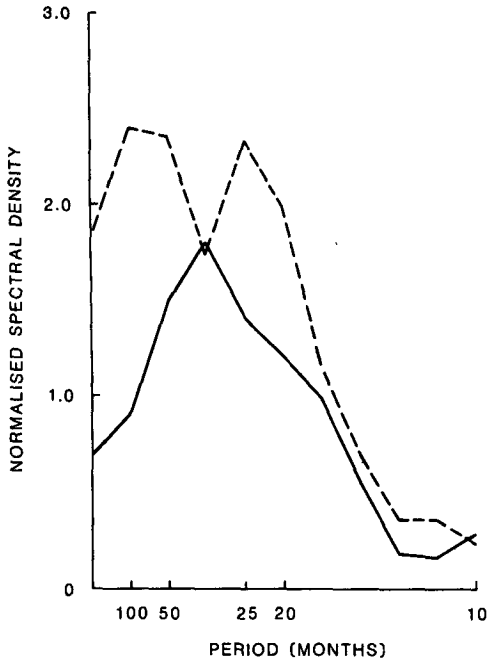

FIG. 8. Spectra of monthly anomalies of observed Darwin pressure (solid lines, 1961–82 data) and simulated pressure (dashed line). Normalization makes the variance of the time series equal to 1.0.

"noise" unrelated to the SO. The observed spectrum has a single peak in the SO range while the simulated series has two peaks, at roughly 5 years and 2 years. Troup (1965) shows a similar double-peaked effect in a spectrum of Darwin pressure from 1921 to 1962.

Spectra of Indonesian SST were not calculated because of the rather short (18 years) time series of uninterrupted data available.

3. A possible mechanism for the El Niño–Southern Oscillation phenomenon

The above comparison of the correlations, spectra and standard deviations calculated from the simulated anomalies with those calculated from observed anomalies in the Indonesian–north Australian area (Figs. 3–7) indicates that the model can reproduce rather well the complex statistical behavior of these observed anomalies.

The typical signal in Darwin pressure and Indonesian SST associated with the El Niño should, therefore, also be reproducible by the model, since large anomalies of pressure and SST in the Indonesia–north Australia region are often associated with El Niño events. Rasmusson and Carpenter (1982) calculated composites of several atmospheric and oceanic variables from a larger number of El Niño years. Some of their results are shown in Fig. 9 (also see Fig. 1). The solid line in Fig. 9 shows three-month running means of Darwin pressure (from their Fig. 15) while the large dots represent an estimate of their composite SST anomaly at 5°S, 125°E from their Figs. 17–23. The composite Darwin pressure anomaly shows a maximum at about September–November in the year of an El Niño. Therefore, composites of simulated pressure and SST anomalies have been calculated for the five years in Fig. 2a when the simulated pressure anomalies reached maximum positive values for the period September–November and are plotted in Fig. 9.

The composites computed from the simulated data match closely the composites from the observed data, i.e., the model can reproduce the observed sequences of anomalies of Indonesian SST and Darwin pressure around the time of El Niño events. If a physical process existed which was representable by the model equations, this process could be proposed as a possible cause of the observed behavior of Indonesian SST and Darwin pressure anomalies associated with ENSO events. A physical process which appears plausible and representable by the model equations is suggested below. Essentially, it is postulated that local, stochastically-forced and seasonally-varying air–sea interaction in the Indonesian region may provide the physical basis. The postulated process does not involve the effects of events outside the Indonesian region in the generation of Indonesian region anomalies.

Gill (1980) used a simple analytic model to examine the likely response of the tropical atmosphere to equatorial diabatic heating. He concluded that heating would result in decreased pressures over and around the area of heating. Gill's results suggest that a warmer than normal SST in the Indonesian region, through diabatic heating of the atmosphere, would lead to a decrease in atmospheric pressure. The same result was found by Keshavamurty (1982) in a study of the response of a general circulation model of the atmosphere to the insertion of a warm SST anomaly in the Indonesian region (his Fig. 6). Similar results have also been presented by Matsuno (1966), Webster (1972).

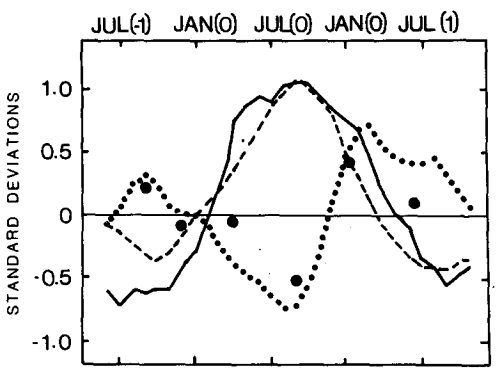

FIG. 9. Composites of three-month running means of Darwin pressure anomalies (solid line) and SST anomalies at 5°S, 130°E (large circles) near years of El Niño (from Rasmusson and Carpenter, 1982). Also shown are composites of three-month running means of pressure (dashed line) and SST (dotted line) in the five years from Fig. 10 when September–November simulated pressure was a maximum.

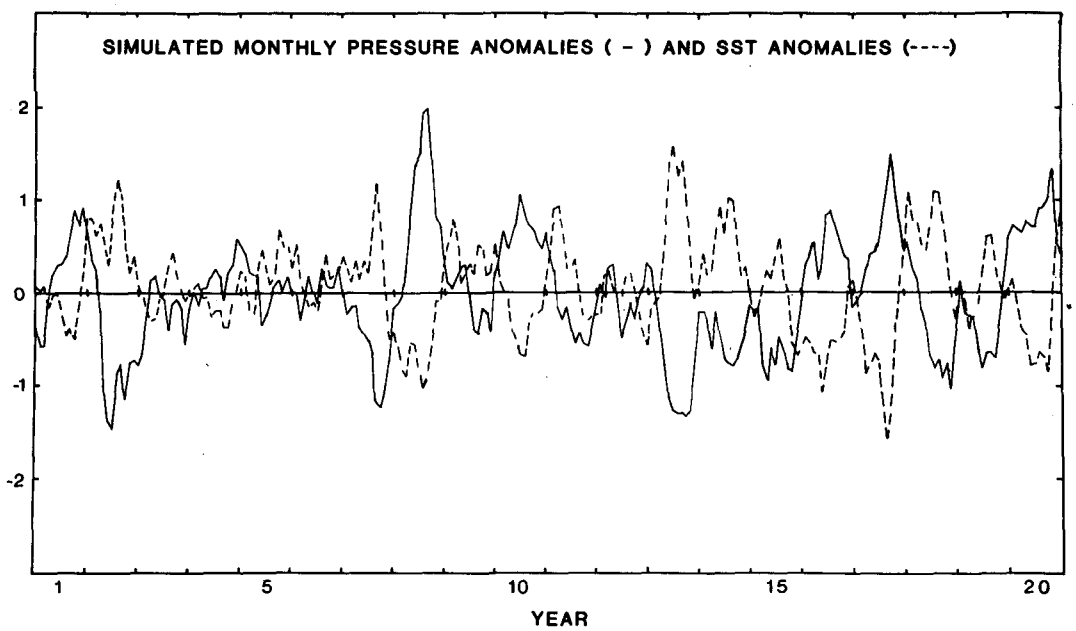

FIG. 10. Time series of monthly means of pressure (solid line) and SST (dashed line) produced by the model. January of each year is indicated.

and Rowntree (1972), using a variety of approaches. Eq. (1) can be interpreted as representing this tendency for a warm SST anomaly (T) to reduce pressure (P) in the surrounding area.

In order to advance an interpretation of the physical meaning of Eq. (2), it is necessary to examine the response of the low-level wind field to an SST anomaly, again using the results of Gill and of Keshavamurty. Gill's Fig. 1 indicates that the diabatic heating results in the formation of westerlies over and to the west of the heating, with easterlies to the east. Keshavamurty's Figs. 7, 9 and 13 indicate that anomalous low-level westerlies occur over and to the west of the SST anomaly, again with easterly anomalies to the east of the SST anomaly. It seems likely that these anomalous westerlies would have an effect on the SST anomaly that produced them in the first place. It is suggested that the actual effect will depend on the direction of the prevailing wind. In the Indonesian region, the prevailing wind over the period from April to September is basically easterly, becoming westerly the rest of the year. Thus, depending on the time of year, the anomalous westerly wind produced by a warm SST anomaly in the Indonesian region will have the effect of either strengthening the prevailing wind (October–March) or weakening it (April–September).

These two different situations may have different effects on the initial warm SST anomaly. It seems possible that an increase in wind strength may result in increased mixing of the upper ocean, leading to a deepening of the mixed layer and increased entrainment across the thermocline. In turn this may lead to a decrease in the SST. On the other hand, a lower wind speed may result in warming of the SST. If so, then the initial warm SST anomaly, if it occurred during April–September, would produce a response of decreased atmospheric pressure and weak winds which would, in turn, allow the SST to rise farther. Thus, the negative anomaly in pressure would be associated with a tendency for an increase in SST, due to reduced wind speed.

If the initial warm SST anomaly occurred during October–March, the atmospheric response would again be decreased pressure but also an increased wind speed over the SST anomaly. This increase on the wind should induce increased mixing and thus a cooling of the initial SST anomaly. Therefore, in this season, in contrast to the April–September season, low atmospheric pressure would be associated with a tendency for SST to decrease.

If the mechanism outlined above does take place, it could explain the seasonal variation in the effect of P on T in Eq. (2). In this equation, during April–September, a negative P tends to increase T, whereas during October–March, it tends to decrease it. The converse applies for positive values of P.

This discussion has attempted to show that a plausible physical basis for Eqs. (1) and (2) can be advanced. Implicit in the postulated mechanism is that wind-induced mixing of the upper ocean is an important mechanism affecting SST in the Indonesian region. Other processes (e.g. heating and advection) presumably also affect the SST. It is important to determine the importance of these various processes, relative to wind-induced mixing. Observational and modeling studies of Indonesian SST and its relationship to the atmosphere appear necessary to fully establish the plausibility of the model. The plausibility of the hy-

pothesis also depends on whether the values of the constants in the equations are reasonable, although, as noted earlier, a range of values exists for which the model produces SO-like sequences. The hypothesis clearly requires validation by further empirical, statistical and modeling studies.

If the postulated physical process were valid, this would suggest that ocean–atmosphere interaction might be the cause of the initiation, growth and destruction of the observed atmospheric and oceanic anomalies in the Indonesian region. The close relationship (Figs. 1 and 9) observed between these anomalies and atmospheric and oceanic anomalies associated with the ENSO in other regions (e.g., the east equatorial Pacific) in turn leads to the conclusion that these other manifestations of the ENSO might be forced by this interaction in the Indonesian region. The evidence presented earlier suggests that SST in this region tends to decrease (possibly as a result of the postulated interaction) around October–November in the year prior to the appearance of warm SST in the east Pacific. Such a decrease in Indonesian SST should, according to Gill (1980) and many others, tend to weaken the easterlies immediately east of the Indonesian SST anomaly (i.e., over the west equatorial Pacific) leading eventually to a warming of the east Pacific, through the mechanism described in Section 1. These low Indonesian SST's and the west equatorial Pacific easterly wind anomalies would then be maintained through the Southern Hemisphere winter by the positive feedback in the Indonesian region. Around October–November, the Indonesian SST's rise dramatically, again as a consequence of the seasonally-varying feedback, initiating anomalously strong easterly flow in the area just to the east i.e., over the west equatorial Pacific. The appearance of these strong easterly anomalies is a precursor of the collapse of the El Niño anomaly early the following year (Rasmusson and Carpenter, 1982).

Thus, it might be that the Indonesian region interaction postulated here is the "cause" of many facets of the El Niño, including its phase-locking to the annual cycle and its typical time scale of about a year.

4. Concluding remarks

This study has demonstrated 1) that Indonesian SST anomalies are closely related to the ENSO phenomenon and 2) that the behavior of these anomalies and that of atmospheric anomalies in this region can be reproduced to a considerable degree by a very simple *ad hoc* model. It has been suggested that the model can be interpreted as representing some form of stochastically-forced, seasonally-varying interaction between the atmosphere and ocean in the Indonesia–north Australia region, with no inclusion of the effects of events outside this region. A possible physical basis for such an interaction has also been postulated. Such interaction, it is suggested, produces large anomalies in the atmosphere and ocean in the Indonesian region, including the generation of zonal wind anomalies over the west equatorial Pacific. Such anomalies are generally regarded as the precursors of El Niño events and it has therefore been suggested that the postulated interaction in the Indonesian region might be the cause of certain aspects of the El Niño–Southern Oscillation phenomenon.

The proposed mechanism, if valid, could explain such features as the close and seasonally-varying links between Indonesian SST and ENSO; the sudden appearance of westerly wind anomalies in the west equatorial Pacific and their sudden replacement by easterly anomalies about 12 months later; the time of year such changes preferentially occur; the typical time scale of ENSO anomalies of about 12 months; the tendency for SO anomalies to be preceded and followed by extended periods of anomalies of the reverse sign; and the apparent randomness in the period between successive El Niño anomalies. All these features of ENSO anomalies can be explained by the postulated interaction in the Indonesian region alone, simply by regarding the equatorial Pacific ENSO anomalies as the dynamic response to Indonesian anomalies produced by this interaction.

Of course other, presumably more complicated, mechanisms could also be advanced to explain the complex set of relationships between observed Indonesian SST anomalies and ENSO. The explanation advanced here is clearly speculative and its very simplicity suggests that other effects will need to be taken into account to provide a complete mechanism for the ENSO phenomenon.

Irrespective of the *cause* of ENSO events, the results of this study are of interest for the *prediction* of such events. In particular, it appears that Indonesian SST anomalies decrease some months prior to the initial appearance of El Niño in the east Pacific and prior to the increase in Darwin pressure anomaly associated with the ENSO phenomenon. Similarly, a rapid increase in Indonesian SST anomaly appears to signal the end of the ENSO event, this increase again occurring around October–November, several months before the SST anomaly in the east equatorial Pacific disappears. If this is correct, and the cross correlation and serial correlation analysis of the observed data (Section 2) as well as the composites of Rasmusson and Carpenter (1982) support this scenario, monitoring of the Indonesian SST's could provide a better means of predicting El Niño than the use of pressure-based SO indices such as those proposed by Quinn (1974).

Acknowledgments. P. B. Wright kindly provided the 1964–82 SST data. K. E. Trenberth made many suggestions to improve the manuscript.

REFERENCES

Barnett, T. P., 1983: Interaction of the monsoon and Pacific trade wind system at interannual time scales. Part I: The equatorial zone. *Mon. Wea. Rev.*, **111**, 756–773.

Berlage, H. P., 1957: Fluctuations of the general atmospheric circulation of more than one year, their nature and prognostic value. *Medel. Verhandel.*, **69,** Konink. Nederlands Meteor. Inst., 152 pp.

Busalacchi, A. J., and J. J. O'Brien, 1981: Interannual variability of the equatorial Pacific in the 1960's. *J. Geophys. Res.*, **86,** 10901–10907.

Chen, W. Y., 1982: Assessment of Southern Oscillation sea-level pressure indices. *Mon. Wea. Rev.*, **110,** 800–807.

Gill, A. E., 1980: Some simple solutions for heat-induced tropical circulation. *Quart. J. Roy. Meteor. Soc.*, **106,** 447–462.

Hurlburt, H. E., J. C. Kindle and J. J. O'Brien, 1976: A numerical simulation of the onset of El Niño. *J. Phys. Oceanogr.*, **6,** 621–631.

Keshavamurty, R. N., 1982: Response of the atmosphere to sea surface temperature anomalies over the equatorial Pacific and teleconnections of the Southern Oscillation. *J. Atmos. Sci.*, **39,** 1241–1259.

Matsuno, T., 1966: Quasi-geostrophic motions in the equatorial area. *J. Meteor. Soc. Japan,* **44,** 25–43.

McCreary, J., 1976: Eastern tropical ocean response to changing wind systems: with application to El Niño. *J. Phys. Oceanogr.*, **6,** 632–645.

——, 1983: A model of tropical ocean–atmosphere interaction. *Mon. Wea. Rev.*, **111,** 370–387.

McWilliams, J. C., and P. R. Gent, 1978: A coupled air–sea interaction model for the tropical Pacific. *J. Atmos. Sci.*, **35,** 962–969.

Newell, R. E., R. Selkirk and W. Ebisuzaki, 1982: The Southern Oscillation: Sea surface temperature and wind relationships in a 100-year data set. *J. Climatol.*, **2,** 357–373.

Nicholls, N., 1979: A simple air-sea interaction model. *Quart. J. Roy. Meteor. Soc.*, **105,** 93–105.

Philander, S. G. H., 1983: El Niño Southern Oscillation phenomena. *Nature,* **302,** 295–301.

Priestley, C. H. B., 1962: Some lag associations in Darwin pressure and rainfall. *Aust. Meteor. Mag.*, **38,** 32–42.

Quinn, W. H., 1974: Monitoring and predicting El Niño invasions. *J. Appl. Meteor.*, **13,** 825–830.

Rasmusson, E. M., and T. H. Carpenter, 1982: Variations in tropical sea surface temperature and surface wind fields associated with the Southern Oscillation/El Niño. *Mon. Wea. Rev.*, **110,** 354–384.

Rowntree, P. R., 1972: The influence of tropical east Pacific Ocean temperatures on the atmosphere. *Quart. J. Roy. Meteor. Soc.*, **98,** 290–321.

Schregardus, M. W. F., 1938: Sea surface temperature on some steamer routes in Netherlands India. Verhandel. No. 28, Konink. Magnet. Meteor. Observ. Batavia, Indonesia, 22 pp.

Trenberth, K. E., 1976: Spatial and temporal variations of the Southern Oscillation. *Quart. J. Roy. Meteor. Soc.*, **102,** 639–653.

——, 1984: Signal versus noise in the Southern Oscillation. *Mon. Wea. Rev.*, **112,** 326–332.

Troup, A. J., 1965: The Southern Oscillation. *Quart. J. Roy. Meteor. Soc.*, **91,** 490–506.

Webster, P. J., 1972: Response of the tropical atmosphere to local steady forcing. *Mon. Wea. Rev.*, **100,** 518–541.

Wright, P. B., 1979: A simple model for simulating regional short-term climatic changes. *Mon. Wea. Rev.*, **107,** 1567–1580.

Wyrtki, K., 1975: El Niño—the dynamic response of the equatorial Pacific Ocean to atmospheric forcing. *J. Phys. Oceanogr.*, **5,** 572–584.

——, 1979: The response of sea level topography to the 1976 El Niño. *J. Phys. Oceanogr.*, **9,** 1223–1231.